THE AMERICAN SOCIETY OF MECHANICAL ENGINEERS
345 E. 47 St., New York, N.Y. 10017

85-GT-218

Axial Flow Contra-Rotating Turbines

J. F. LOUIS
Department of Aeronautics and Astronautics
Massachusetts Institute of Technology
Cambridge, MA 02139

ABSTRACT

Two types of contra-rotating stages are considered; the first uses guide vanes and the second is vaneless. The wheels of the first type use bladings which are mirror images of each other and they operate with inlet and outlet swirl. The second type uses dissimilar bladings in each of the two wheels with axial inlet velocity to the first wheel and axial outlet velocity for the second wheel. An analysis of their performance indicates that both types can reach stage loading coefficients comparable or larger than conventional turbines with the same number of wheels. A comparison of the contra-rotating stages with conventional ones indicate a significant stage efficiency advantage of the contra-rotating over the conventional single rotation stages due mainly to the elimination of stationary vanes. The off-design performance indicates that relative wheel speed must be controlled. The attributes of contra-rotating turbines suggest their potential use in high performance aircraft engines, in dynamic space power systems and in low speed industrial gas turbines.

1. INTRODUCTION

Although radial flow contra-rotating steam turbines were built as early as 1913 by Ljungstrom, little mention is made of axial flow contrarotating turbines. However, it is said that machines of this type were built in the U.K. and the U.S. Very recently, the development of an unducted fan engine using a multi-stage contra-rotating turbine was announced.

The contra-rotating turbine under consideration is an axial flow stage comprising two wheels rotating at the same speed and equal torque but in opposite directions (Fig. 1). Under these conditions, the swirl entering the first wheel has to be equal to the swirl leaving the second wheel. Such a turbine could make use of existing two-spool technology and can be considered as the building block of a multistage contra-rotating turbine.

The main apparent attributes of the contra-rotating turbine are:

1) The increase of work per unit mass flow resulting from the large changes in angular momentum made possible by the large relative rotational velocity.

2) The elimination of stator vanes between wheels reduces the weight of the stage, and increases the stage efficiency since it eliminates the pressure drop, leakage and the cooling losses normally associated with vanes.

3) The stage can be torqueless and eliminate gyroscopic effects.

4) Negligible erosion rate through practical low speed operation.

5) Reduction of particulates deposition through control of surface shear flow.

It was recently found that an analysis [1] of two-stage counterrotating turbine efficiencies in terms of work and speed requirements was made for wheels operating at different rotational speeds and with different inlet and outlet swirls. The analysis indicated the efficiency advantage was due to the elimination of the interstage stator. The analysis was concerned with the use of conventional blading in a contra-rotating stage.

This analysis deals with two types of stages designed especially for contra-rotation. The first type uses inlet guide vanes when it operates as a single or first stage and the second is always vaneless. The wheels of the first type are mirror images of each other, the pressure ratio across each wheel is identical and each wheel operates with the same inlet and outlet swirl. The second type uses dissimilar bladings in each wheel, with an axial inlet velocity into the first wheel axial and an axial velocity out of the second wheel. The pressure ratio across the first wheel is larger than

Presented at the Gas Turbine Conference and Exhibit
Houston, Texas — March 18-21, 1985

it is across the second wheel. This stage is an example of contra-rotating stages with dissimilar bladings in each wheel operating with identical swirls entering and leaving the stage.

The purpose of this paper is to evaluate the design and off-design performance of such turbines designed for contra-rotation and to assess the fundamental issues raised by such a stage. A comparison is also made between the performance and stage efficiency of conventional single rotation and contra-rotating stages.

2. CONTRA-ROTATING TURBINE STAGE WITH INLET GUIDE VANES

This stage is made up of a row of inlet guide vanes and of two wheels (a) and (b) rotating in opposite direction with the same rotational velocity (U). The two wheels have bladings which are the mirror image of each other as sketched in Figure 2.

2.1 DESIGN PERFORMANCE

Figure 2 gives the velocity triangles. At design conditions the wheel speeds are equal, or $U_a = U_b = U$. The following conditions exist between angles; $\beta_{a2} = \beta_{b3} = \beta$, and $\beta_{a1} = \beta_{b2}$ and, $\alpha_1 = \alpha_2 = \alpha_3 = \alpha$. It can also be assumed that the axial component of velocity (V_x) is constant throughout the stage. The condition of contra-rotation, is

$$V_x(\tan\beta - \tan\beta_{b2}) = 2U, \quad (1)$$

The total enthalpy change across each wheel can be written as

$$\Delta h_a = \Delta h_b = 2UV_x \tan\alpha = 2U(V_x \tan\beta - U) \quad (2)$$

The total enthalpy drop across the contra-rotating stage is;

$$\Delta h_s = \Delta h_a + \Delta h_b = 4U\ (V_x \tan \beta - U) \quad (3)$$

The stage load coefficient for the contra-rotating stage can be written as:

$$\Psi = \Delta h_s/U^2 = 4(\Phi \tan\beta - 1) = 4\Phi \tan\alpha \quad (4)$$

where $\phi = v_x/u$ is the flow coefficient.

The stage load coefficient is plotted as a function of the flow coefficient in Figure 3 for different values of the outlet angle α. It can be seen that large values of Ψ are achievable for moderate values of α and ϵ_R; ϵ_R is defined as the flow deflection angle in the rotor. Figure 4 gives the flow deflection angle in the rotor as a function of the flow coefficient for different values of α. For a given relative tangential velocity $V_x \tan\beta$, equation 3 maximizes for;

$$U = V_x \tan\beta/2. \quad (5)$$

When this condition is satisfied, $\Psi = 4$ and $\beta_{a1} = \beta_{b2} = 0$.

In order to obtain a better insight, the contra-rotating stage can be compared with a 100% reaction stage having identical guide vanes and wheel blading (Figure 2). In a 100% reaction stage, there is no net pressure drop in the stator and all the pressure drop occurs in the rotor. Since $\beta_{a1} = \beta_{b2}$ in the contra-rotating stage, eq. (1) is identical to the condition satisfied in the 100% reaction stage;

$$V_x(\tan\beta - \tan\beta_{a1}) = 2U.$$

Since equation 2 is equally valid for the 100% reaction stage, equations 3 and 4 also describe the performance of two 100% reaction stages. As shown in Figure 2, the contra-rotation eliminates the stator vanes between the two wheels of a two stage 100% reaction turbine of a single rotation design. The significant pressure losses associated with this large flow deflection, $\epsilon_s = 2\alpha$, in the stator, and the mandatory exit swirl make the single rotation 100% reaction stage turbines unattractive.

2.2 EXAMPLES OF LOCAL DESIGN AND PERFORMANCE

A contra-rotating stage is designed for $\Psi = 4.0$ and $\beta = 70°$. For this condition, $\phi = 0.73$ and $\alpha = 54°$ with $\beta_{a1} = \beta_{b2} = 0$. Although this stage operates with a high load coefficient, the flow deflections through the guide vanes and the wheels are moderate. This indicates favorable aerodynamics for the contra-rotating stage as compared to other turbine designs with identical loading. Comparable 100% reaction stages would have the same wheel design and stator vanes with a flow deflection $\epsilon_s = 108°$. Comparable impulse stages would have a flow deflection of 70° in the stator vanes and 108° in the rotor.

A helium turbine stage using these design parameters together with an inlet temperature of 1300K, a rotational velocity U = 500 m/s and a polytropic efficiency of 90% would have a pressure ratio of 1.55. A combustion turbine stage with the same design parameters together with an inlet temperature of 1500K, a rotational velocity of 450 m/s and a polytropic efficiency of 90% would have a pressure ratio of 15.2. Both of these designs provide high pressure ratios.

A combustion turbine of very low rotational velocity, 100 m/s, designed for the same design parameters and an inlet temperature of 1200°K would have a pressure ratio of 3.39 per stage or 1.84 per wheel. Using a conservative scaling law (2) of erosion rate with velocity, it is estimated that the erosion rate in this turbine should be close to 1/50 of the rate observed in a conventional turbine operating at 300 m/s, all other conditions being equal. The high pressure drop through the wheel should assure the existence of sufficient shear forces around the blading to sweep the particulates, which would otherwise deposit by turbulent diffusion and thermopheresis, from the blades. Such a low velocity contra-rotating turbine could therefore be tolerant to flows with particulates as long as the particles are not sticky.

These high pressure ratios or large work per stage are characteristic of this type of contra-rotating turbine.

2.3 EFFICIENCY OF AN ADIABATIC STAGE USING A CONTRA-ROTATING TURBINE WITH VANES

The design of turbines results from a reasonable compromise between performance, weight, cost and efficiency. The previous evaluation of the contra-rotating turbine stage has indicated that this stage could have both a performance and weight advantage over conventional turbine stages of similar efficiency.

The elimination of stator vanes, which gives a weight advantage, will also result in a reduction of pressure drop losses and therefore a net efficiency gain. A first evaluation of this efficiency gain due to the elimination of the vanes can be obtained by comparing the efficiency of a single contra-rotating wheel with the efficiency of an impulse stage operating with the same stage loading and flow coefficients.

For the case of zero tip leakage, the stage efficiency of an impulse stage can be written as

$$\eta_{T\,impulse} = \frac{1}{1 + \dfrac{\xi_S \phi^2 (1+\tan^2\alpha_2) + \xi_R \phi^2 (1+\tan^2\beta_3)}{2\psi}} \qquad (6)$$

where ξ_S and ξ_R are the loss coefficient of the vanes and blades respectively, and α_2 and β_3 are the flow leaving angles from the vanes and from the blades respectively.

For a wheel of a contra-rotating stage.

$$\eta_{TW} = \frac{1}{1 + \dfrac{\xi_W \phi^2 (1+\tan^2\beta)}{2\psi}} \qquad (7)$$

Since ϕ and ψ are the same for the two wheels, the flow in the vanes of the impulse stage is identical to the relative flow in a contra-rotating wheel so that $\alpha_2 = \beta$ and $\xi_S = \xi_W$.

Therefore, the ratio of the contra-rotating wheel efficiency to the efficiency of the impulse stage can be written, neglecting second order terms, as

$$\frac{\eta_{TW}}{\eta_{T\,impulse}} \simeq 1 + \frac{\xi_R \phi^2 (1+\tan^2\beta_3)}{2\psi} \simeq 1 + \frac{\xi_R \phi}{2\sin\varepsilon} \qquad (8)$$

Where ε is the deflection angle in the impulse wheel.

Since ξ_R is strongly dependent on the deflection angle (which is larger in highly loaded wheels) the contra-rotating stage has a significant efficiency advantage which increases with both stage loading and flow coefficient.

As an example, an impulse stage designed for $\psi = 2.0$, $\phi = 0.73$ and having a deflection of 108° is compared to a single wheel of a contrarotating stage operating at the same conditions of $\psi = 4$ and $\phi = 0.73$. The loss coefficient of the impulse wheel can be reasonably assumed to be $\xi_R = 0.74$. The ratio of efficiencies is determined to be:

$$\frac{\eta_{TW}}{\eta_{T\,impulse}} = 1.029$$

which corresponds to an efficiency advantage of the contra-rotating turbine over the impulse turbine close to 3%.

However, this comparison does not include the influence of the guide vanes on the efficiency of a full contra-rotating stage, which can be written as

$$\eta_{TCR} = \frac{1}{1 + \dfrac{\xi_N \phi^2 (1+\tan^2\alpha_1) + 2\xi_W \phi^2 (1+\tan^2\beta)}{8\phi\tan\alpha_1}} \qquad (9)$$

In order to reach a more thorough understanding of the differences in performance and efficiency of the contra-rotating stage when compared to single rotation conventional stages, carpet maps of the stage efficiencies have been prepared and superimposed on the performance plots. These plots give ψ, the stage loading coefficient, as a function of ϕ, the flow coefficient.

Smith (3) developed such a carpet plot of efficiency, free of leakage losses, measured on model turbines of a family of aircraft engines. An analysis of the correlation of the data indicated that the losses were primarily attributable to the profile and secondary flow losses in bladings of large to moderate aspect ratios used in this family of 50% reaction turbines. Several authors (4,5,6) have tested their loss models by calculating the efficiency of a multitude of turbines similar to those tested by Smith. This mode of calculation is a very laborious process. In this study, a loss model based on a correlation function will be first validated against Smith's data and then used for the evaluation of contra-rotating and conventional turbines. A loss model suggested by Hawthorne[(7)] is used. It is based on the data of Soderberg given in Ref. (7). For a Reynold's number of 2.10^5. The loss factor is written as

$$\xi = 0.017\,[1+(\tfrac{\varepsilon}{90})^2\,][1+3.2\ b/H] \qquad (10)$$

where H/b is the aspect ratio and ε is the flow deflection. The aspect ratio of these turbines was large to moderate and it can be reasonably assumed that the aspect ratio decreased for large flow coefficients. The aspect ratio was around 4.0 for the many turbines designed for flow coefficients in the range of 0.6 to 0.7. Following Hawthorne,[(7)] it is assumed that

$$H/b = 2.5/\phi. \qquad (11)$$

Using equations (10) and (11), the efficiency of 50% reaction turbines can be evaluated and the results can be compared with the data of Smith. Considering the scatter of the experimental data, the overall agreement between prediction and data is quite good and it justifies the use of relations (10) and (11) in the evaluation of efficiencies for both the contra-rotating and the single rotation turbines. Fig. 6 gives the stage efficiency of the contra-rotating turbine stage with guide vanes and Fig. 7 gives the efficiency of a conventional impulse stage. A general comparison indicates that the efficiency advantage of the contra-rotating turbine increases with stage loading coefficient and to a lesser extent with flow coefficient. For example, for a flow coefficient $\phi = 0.6$ and a one wheel loading coefficient of $\psi = 1.5$, (3 for a contra-rotating stage made of two wheels) the stage efficiency is $\eta = 94.8\%$ for the impulse stage, $\eta = 93.0\%$ for the 50% reaction stage and $\eta = 95.3\%$ for the contra-rotating stage. This reveals a 1.5% or better efficiency advantage of the contra-rotating stage over the other two single rotation designs. For the same flow coefficient $\phi = 0.6$ and $\psi = 2.0$ (4.0 for the complete contra-rotating stage), the stage efficiency is $\eta = 92.3\%$ for the impulse stage, $\eta = 91.3\%$ for the 50% reaction stage and 94.2% for the contra-rotating stage, an efficiency advantage of at least 1.9% for the contra-rotating stage over the other two. This efficiency advantage increases with both ψ and ϕ.

Modern engines have made significant improvements in component efficiencies since the time of Smith's work. A valid loss model for the most recent engines is not readily available, it would no doubt result in higher turbine efficiencies but the relative advantage of the contra-rotating turbine would remain the same as indicated by equation (8).

In high pressure ratio stages the flow can become supersonic and Mach losses can ensue. Let us examine the influence of Mach losses on the efficiency comparison between contra-rotating and impulse stages. For equal work, the total temperatures behind each wheel are equal for the two turbines. Since

$$\alpha<\alpha_{2impulse} \text{ and } V_2<V_{2impulse} \qquad (12)$$

and the static temperatures in the contra-rotating stage are higher than the corresponding temperatures in the impulse stages. Considering the equality of velocities,

$$V_{1\ impulse} = W_2 \text{ and } W_{2\ impulse} = V_1 = V_2 \qquad (13)$$

the associated Mach numbers are lower in the contra-rotating stage than in the impulse stages which implies that the Mach losses in an impulse stage should be larger than for the contra-rotating stage of equal performance. It is apparent that the contra-rotating turbine has a significant efficiency advantage over the impulse machine of identical output, and this advantage can be even greater for cooled turbines.

2.4 LOCAL OFF-DESIGN PERFORMANCE

In the evaluation of the off-design performance, we can assume that the relative leaving angles, α and β, remain constant. The enthalpy extraction from each wheel can be written as:

$$\text{Wheel (a):}\quad \Delta h_a = U_a\,[V_{x1}\tan\alpha + V_{x2}\tan\beta - U_a] \qquad (14)$$
$$\text{Wheel (b):}\quad \Delta h_b = U_b\,[V_{x2}\tan\beta - U_a + V_{x3}\tan\beta - U_b] \qquad (15)$$

In order to achieve $U_a = U_b$ and $\Delta h_a = \Delta h_b$, the following condition must be satisfied.

$$\tan\alpha = \frac{V_{x3}}{V_{x1}}\tan\beta - \frac{U}{V_{x1}} \qquad (16)$$

This condition indicates that the guide vanes would have to be variable if the wheel speeds were not controlled. When the above relationship is satisfied the off-design enthalpy extraction is

$$\Delta h_s = U\,[2(V_{x2} + V_{x3})\tan\beta - 4U] \qquad (17)$$

Since $\tan\beta = 2\left(\frac{U}{V_x}\right)_D$ and we define $\bar{V} = \frac{V_{x2} + V_{x3}}{2}$ (18)

Revealing that the loading coefficient is linearly dependent on the flow coefficient.

$$\psi = \frac{\Delta h_a + \Delta h_b}{U^2} = 4\,[2.\left(\frac{U}{V_x}\right)_D \left(\frac{V_x}{U}\right) - 1]$$

For example when, $\left(\frac{\bar{V}_x}{U}\right)_D = 0.73$ (or $\beta = 70°$)

$$\psi = 4[\frac{2}{0.73}\cdot\frac{\bar{V}}{U} - 1]$$

The changes in guide vane outlet angle (α) required to maintain equal work from each of the two wheels are small. The angle can vary from α = 54° at design to α = 64° for a flow coefficient varying between .73 and 1.5. Other types of control can be considered depending on the application.

2.5. DESIGN OF A CONTRA-ROTATING STAGE WITH GUIDE VANES

Section 2.2 dealt with the local design considerations applicable to high hub/tip ratio stages. In this section, the design of stages of lower hub/tip ratios is considered. Constant work is assumed along the radius. Under this assumption, the load coefficient is highest at the hub section of the wheels. This condition of constant work can be written;

$$2UV_x\tan\alpha = 2U(V_x\tan\beta - U) = U_h^2\cdot\Psi_h/2 \qquad (19)$$

where Ψ_h is the stage load coefficient at the hub section.

Using (19) we can write,

$$\tan\beta = \frac{\Psi_h}{4\phi_h}\left(\frac{r_h}{r} + \frac{2}{r_h}\right) \qquad (20)$$

and

$$\tan\alpha = \frac{\Psi_h}{4\phi_h}\cdot\frac{r_h}{r} \qquad (21)$$

The constant work condition along the radius implies constant angular momentum and results in a free vortex design. The relative inlet angle β_1 is derived from

$$\tan\beta_1 = \frac{\Psi_h}{4}\left(\frac{r_h}{r} - \frac{r}{r_b}\right)\frac{1}{\phi_h} \qquad (22)$$

As an example, table I gives the flow angles α, β, and β_1 and the deflection in the rotor $\epsilon_r = \beta_1 + \beta$ for a wheel with a hub to tip ratio of 0.7 and using the conditions: $\Psi_h = 4$, $\phi = 73$, $\beta = 70°$, and $\alpha = 54°$.

TABLE I

r/r_t	α	β_1	β	ϵ_R
0.7	54°	-0	70°	70°
0.8	50°5	-19°5	70°1	50°.6
0.9	47°	-32°2	70°5	38°.3
1.0	43°5	-45°	71.5°	26°.5

The flow and the blading are fairly typical of a free-vortex turbine design with moderate deflection and twist. The blade leaving angle β is almost constant with radius. The deflections decrease with radius, the local efficiency should increase with radius and the blading twist is moderate. The bladings should therefore be relatively easy to manufacture.

3. THE VANELESS CONTRA-ROTATING STAGE

This stage consists of two wheels (a) and (b) with dissimilar bladings rotating at the same velocity (U) in opposite directions. The velocities entering and leaving the stage are axial. The two wheels and associated velocity triangles are sketched in Figure 8.

3.1 DESIGN PERFORMANCE

The axial velocities are assumed constant and the wheel rotational velocities are equal; $U_a = U_b = U$. Since the absolute velocities at the entrance to the stage are axial, the tangential components of the corresponding relative velocities are equal to the rotational velocity or

$$U = V_x.\tan\beta_{1a} = V_x\tan\beta\,a_{3b} \qquad (23)$$

The enthalpy change across the first rotor can be written

$$\Delta h_a = U(V_x.\tan\alpha_2) = U^2(\phi.\tan\beta_{2a} - 1) \qquad (24)$$

and across the second rotor as

$$\Delta h_b = U(V_x.\tan\beta_{2b} + V_x.\tan\beta_{3b}) = U(V_x.\tan\beta_{2b} + U) = U^2(\phi.\tan\beta_{2a} - 1). \qquad (25)$$

The total enthalpy drop across the stage is;

$$\Delta h_s = \Delta h_a + \Delta h_b = 2U^2(\phi.\tan\beta_{2a} - 1)$$

or

$$\Psi=2(\phi.\tan\beta_{2a}-1). \qquad (26)$$

This load coefficient is half the value obtained in equation 4 or is identical to the expression derived for a 100% reaction turbine stage, but these other two stages have significant exit swirl.

Figures 9 and 10 give plots of the load coefficient and flow deflections (ε_a and ε_b) in the wheels as a function of the flow coefficient for different values of β_{2a}. The flow deflections are given by

$$\varepsilon_a=\beta_{2a}-\beta_{1a} \text{ and } \varepsilon_b=\beta_{2b}+\beta_{3b} \text{ with } \tan\beta_{2b}=\tan\beta_{2a}-2/\phi \qquad (27)$$

The first wheel (a) makes use of high stagger blading with moderate deflection whereas the deflection is large in the second wheel (b). The second wheel becomes impulse when $\beta_{2b}=\beta_{3b}$ or using (23) and (28) when

$$\tan\beta_{2a}=3/\phi \qquad (28)$$

When the second wheel is impulse, equation (26) yields a load coefficient of:

$$\Psi=4.$$

A value of the load coefficient of 4 is a practical upper limit for this stage since larger values would entail diffusion in the second wheel.

3.2 EXAMPLE OF LOCAL DESIGN AND PERFORMANCE

Consider a vaneless stage designed for the same conditions as those used in 2.2, namely $\Psi=4$ and $\phi=0.73$. The blading angles are;

$$\beta_{1a}=\beta_{2b}=\beta_{3b}=54°,\ \beta_{2a}=76.3°,\ \varepsilon_a=22.3° \text{ and } \varepsilon_b=108°.$$

This stage is made up of a first wheel with a blading of high stagger and low deflection whereas the second wheel is impulse and is identical to the impulse wheel discussed in 2.2 for the same performance.

The arguments brought forward in 2.4 concerning the off-design performance are also valid for this stage. They indicate the need for a direct speed control such as variable pitch on one of the two wheels or the use of external controls.

3.3 EFFICIENCY OF THE VANELESS STAGE

Assuming adiabatic wheels, the turbine stage efficiency can be written as

$$\eta_T = \frac{1}{1 + [\xi_a w_{2a}^2 + \xi_b w_3^2]/2\,(h_1 - h_3)}$$

$$= \frac{1}{1 + \dfrac{\xi_a\,\phi^2(1+\tan^2\beta_{2a}) + \xi_b(\phi^2+1)}{4(\phi\tan\beta_{2a}-1)}} \qquad (29)$$

The stage efficiency can be computed making the same assumptions as those used in 2.2. The constant efficiency curves are plotted in figure 11. They indicate that high efficiencies can be achieved for different combinations of high load and flow coefficients. A comparison of figure 11 with figure 6 indicates that the vaneless stage has an efficiency advantage over the single rotation stages which increases with load and flow coefficients. This vaneless contra-rotating stage has a significant efficiency advantage over conventional turbine stages of equal performance as discussed in 2.2. This efficiency is derived from the lack of vanes in the stage. However for high pressure ratio applications, the higher Mach losses of the vaneless stage will reduce some of the efficiency advantage described above. For cooled stages, the elimination of stationary vanes and their associated cooling losses results in a further significant efficiency advantage. However, the latter is mitigated by the higher cooling requirement of the first wheel associated with a relative stagnation temperature higher than the absolute total temperature there.

3.4 DESIGN OF A VANELESS CONTRA-ROTATING STAGE

As discussed in section 2.5, constant work is assumed along the radius and the load coefficient achieves its maximum value at the hub, Ψ_h. This condition can be written as

$$U^2(\phi\tan\beta_{2a} - 1) = U_h^2\,\Psi_h/2$$

or

$$\tan\beta_{2a}=[\Psi_h/2\ .\ (r_h/r + r/r_h)]/\phi \qquad (30)$$

The velocity triangles yield;

$$\tan\beta_{1a}=\tan\beta_{3b}=r/r_h.1/\phi \qquad (31)$$

and

$$\tan\beta_{2b}=[\Psi_h/2.(r_h/r - r/r_h)]/\phi \qquad (32)$$

As an example, Table II gives the flow angles and deflections as functions of the radius ratio for a stage designed for $\Psi_h=4$, $\phi=.73$ and a hub to tip ratio of 0.7.

TABLE II

r/r_t	β_{1a},β_{3b} °	β_{2a} °	β_{2b} °	ε_a °	ε_b °
0.7	54	54	54	22.3	108
0.8	57.4	75.8	40	18.4	97.4
0.9	60.5	75.6	19.6	15.1	79.9
1.0	63	75.5	-2.3	12.5	60.7

The first wheel uses a high stagger blading with rather small deflections whereas the second wheel has a nearly constant inlet angle with radius and an appreciable twist. The "degree of reaction" increases from zero at the hub, increasing toward the tip in the second wheel.

4. ROTOR-ROTOR INTERACTION

The large relative velocity between rotors will affect the fluid mechanics and acoustics of the contra-rotating stage.

The acoustics of turbomachinery ducts was first studied by Tyler and Sofrin [8] and the same cut-off condition of noise propagation exists for the sound generated by contra-rotating turbomachinery. (Acoustic modes above the cut-off condition move with an absolute supersonic velocity and propagate without attenuation).

The acoustic modes, generated by one wheel having B blades and turning at an angular velocity Ω due to the interference of an adjacent wheel with B blades and moving at angular velocity Ω_a, have an angular velocity (ω) which can be written as:

$$\omega = \frac{B_a\Omega_a + mB\Omega}{B_a - mB} \qquad (33)$$

where m is an integer (positive or negative).

This relation indicates that the ratio of the number of blades of adjacent wheels should not be integer.

For a conventional turbine, the rotor-stator interaction can be obtained by making $\Omega = 0$ in equation 33 and it yields as in ref. (8)

$$\omega = \frac{B_a \Omega_a}{B_a - mB} \tag{34}$$

The addition of the term, $B\Omega$ in the numerator of equation 34 to yield equation 33 indicates that more acoustic modes are likely to be above the cut-off condition in a contra-rotating turbine than in a conventional turbine operating at the same angular velocity (Ω_a) and making use of a similar number of blades.

The problems of rotor-rotor interaction including the effects of wakes impinging at relatively large negative incidences on the downstream rotor are being treated in detail by Mosca.[9]

5. CONCLUSIONS

1) Two types of contra-rotating stages are considered: the first uses guide vanes when it operates as a single or first stage and the second is vaneless. The first type uses bladings which are the mirror image of each other. The vanes and rotor blading are the same as the bladings which would be used in 100% reaction turbines. The second type, vaneless, uses dissimilar bladings in each of the two wheels with an axial inlet velocity to the first wheel and an axial outlet velocity for the second wheel: the first wheel uses a high stagger and low deflection blading whereas the second wheel has a low stagger and high deflection blading. Both types can reach stage loading coefficients comparable or larger than conventional single rotation turbine stages with the same number of wheels. The first type can be used for high work, whereas the stage loading coefficient of the second type is limited to a stage loading coefficient of four. The second type is an example of contra-rotating stages with dissimilar bladings in each wheel operating with identical swirls entering and leaving the stage. The elimination of the vanes between wheels provides weight, length and performance advantages.

2) The stage efficiency of the contra-rotating turbine is compared to that of conventional impulse and 50% reaction stages. The comparison indicates that the contra-rotating turbines have a substantial efficiency advantage over the conventional stages for moderate pressure ratios. This efficiency advantage is mostly derived from the elimination of stationary bladings and to a lesser degree from the use of moderate deflections in the bladings. In high pressure ratio stages, Mach losses should be smaller in the contra-rotating stage with guide vanes than in the impulse stage of identical performance; but the Mach losses should be higher in the vaneless contra-rotating stage than in the other two types of stages. For turbine stages requiring cooling, the contra-rotating stages will provide a substantial reduction of cooling losses associated with the elimination of stationary vanes which require more cooling than rotating blades. However first wheel of the vaneless stage has an inlet relative stagnation temperature larger than the stagnation temperature based on the absolute velocity. The elimination of the stator vanes should also result in reduced leakage losses.

3) The different attributes of contra-rotating turbines are: high specific power, high efficiency and the possibility of balancing both torques and gyroscopic effects. These attributes suggest the potential use of contra-rotating turbines in high performance aircraft engines, in dynamic space power systems, and in low speed gas turbines designed to be tolerant of particulates in their working fluid.

4) Free vortex blade designs of both types of contra-rotating turbines are relatively easy to manufacture.

5) The off-design performance indicates that controls will be needed to maintain the desired rotor speeds.

6) The elimination of stator vanes brings forth the phenomena associated with rotor-rotor interaction. A preliminary analysis of the acoustic modes generated in a contra-rotating stage indicates that more modes are likely to propagate than in a conventional turbine stage operating at the same angular velocity and with similar number of blades.

5. REFERENCES

1. W.T. Wintucky and W.L. Stewart," Analysis of two-stage counter-rotating turbine efficiencies in terms of work and speed requirements," WACA, RM E57 L05.

2. M. Menguturk and E.F. Sverdrop, Calculated tolerance of a large electric utility gas turbine to erosion damage by coal gas ash particles. p. 193-224 in Erosion, prevention and useful application edited by W.F. Adler. ASTM Special technical publication 664, 1979.

3. Smith, S.F., "A Simple Correlation of Turbine Efficiency", Journal of Royal Aeronautical Society, Vol. 69,, July 1965, pp. 467-470.

4. Dunham, J. and Came, P.M., "Improvements to the Ainleyl/Mathieson Method of Turbine Performance Prediction", ASME Journal of Engineering for Power, July 1970, pp. 252-256.

5. Craig, H.R.M., and Cox, H.J.A., "Performance Estimate of Axial Flow Turbines", Proceedings of the Institution of Mechanical Engineers, Vol. 185, No. 32, 1971, pp. 407-424.

6. Kacker S. C. and Okapuu. U., "A mean line prediction method for axial flow turbine efficiency". Journal of Engineering Power, 1981.

7. J.H. Horlock, "Axial Flow Turbines", Robert E. Krieger, Publishing Company, New York (1966).

8. J.M. Tyler and T.G. Sofrin, 'Axial flow compressor noise studies,' Society of Automotive Engineers Transactions, 70, 309-332, 1962.

9. Mosca, J., "Rotor-rotor interaction in a contra-turbine stage". M.Sc Thesis, May, 1985.

Appendix

NOMENCLATURE

B: number of blades on a wheel
Δh: total enthalfy drop across a stage
H/b: aspect ratio based on blade chord
m: integer related to an acoustic mode
U: rotational velocity of a wheel
V: absolute flow velocity
w: relative flow velocity
α: absolute flow angle measured from the axis
β: relative flow angle measured from the axis
ϵ: flow deflection angle in a blade row
η: stage efficiency
ξ: loss coefficient of a blade row
ω: angular velocity of an acoustic mode
Ω: angular velocity of a wheel
ϕ: flow coefficient
ψ: stage loading coefficient

Subscripts

a first wheel
b second wheel
1 upstream of first wheel
2 between wheels
3 downstream of second wheel
x axial component
s stator
R rotor
r radius
D design condition
h hub
t tip
N nozzle
W Wheel

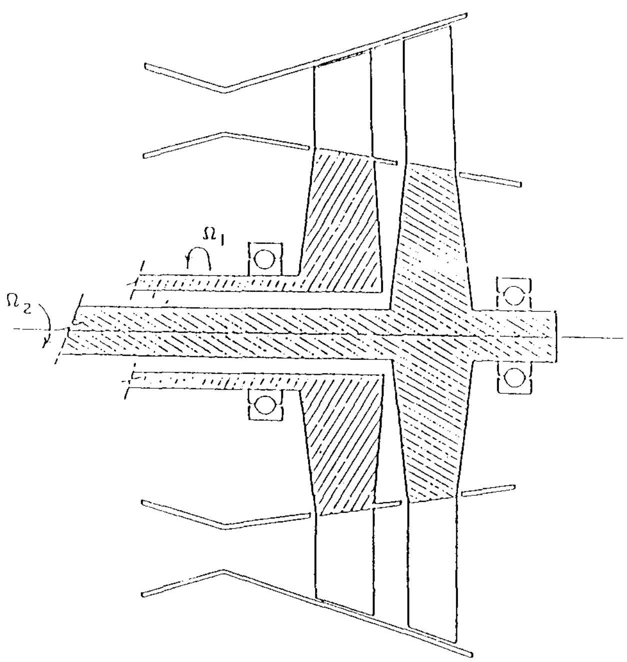

Fig. 1 SKETCH OF AN AXIAL FLOW CONTRA-ROTATING TURBINE

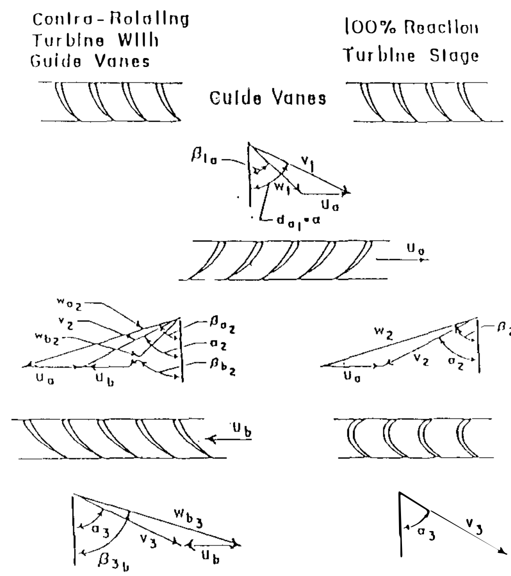

Fig. 2 VELOCITY TRIANGLES IN BOTH A CONTRA-ROTATING STAGE WITH GUIDE VANES AND EQUIVALENT STAGE WITH 100% REACTION

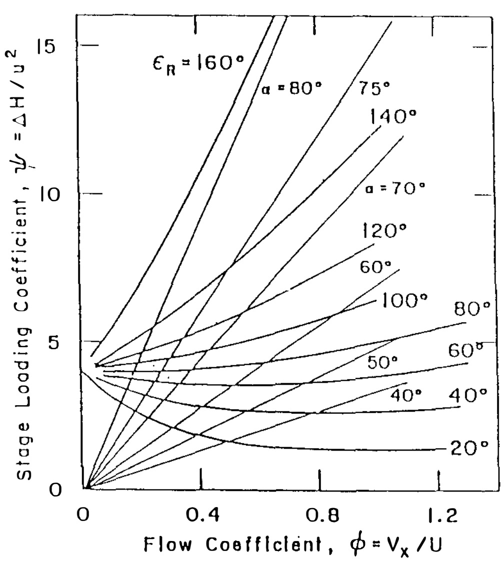

Fig. 3 CHART OF THE STAGE LOADING COEFFICIENT AS A FUNCTION OF FLOW COEFFICIENT FOR A CONTRA-ROTATING TURBINE WITH GUIDE VANES.

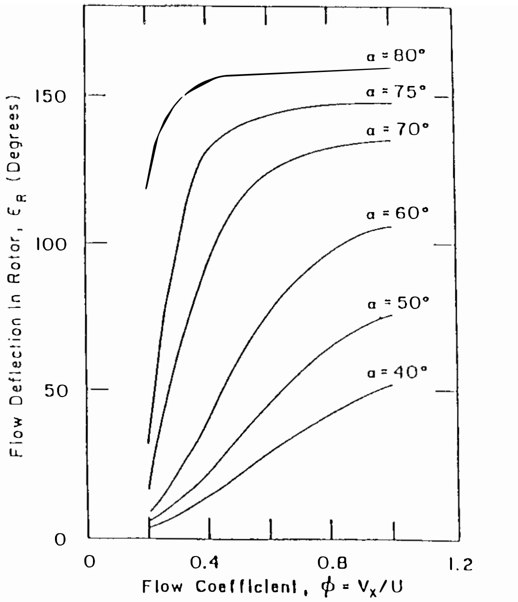

Fig. 4 FLOW DEFLECTION IN ROTORS OF A CONTRA-ROTATING TURBINE SPACE WITH GUIDE VANES AS A FUNCTION OF FLOW COEFFICIENT.

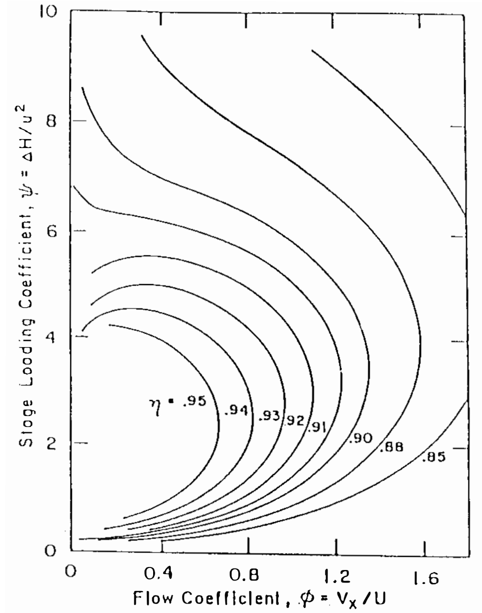

Fig. 6 CHART OF THE STAGE EFFICIENCY OF A CONTRA-ROTATING TURBINE STAGE WITH GUIDE VANES

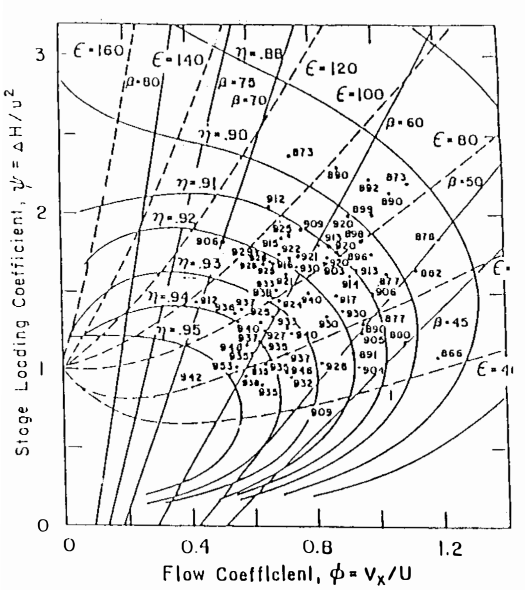

Fig. 5 COMPARISON BETWEEN PREDICTED AND EXPERIMENTAL (Smith) EFFICIENCY DATA FOR 50% REACTION TURBINE USING THE LOSS CORRELATION $\xi = 0.017$

$$\left[(1 + (\frac{\varepsilon}{90})^2\right] [1 + 3.2b] \text{ WITH } \frac{H}{b} = \frac{2.5}{\phi}$$

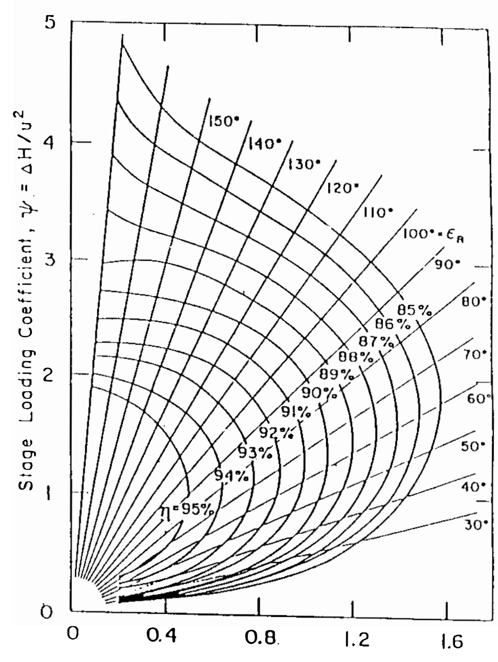

Fig. 7 CHART OF THE STAGE EFFICIENCY OF SINGLE ROTATION IMPULSE TURBINE STAGE

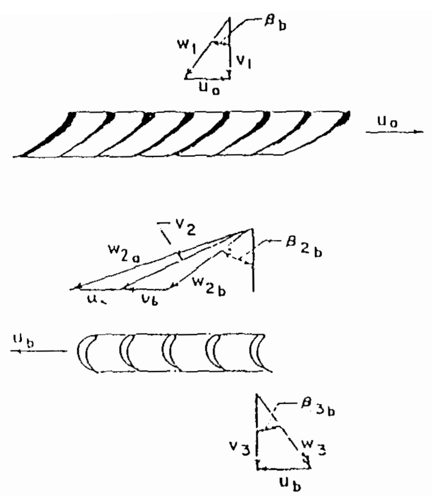

Fig. 8 VELOCITY TRIANGLES IN A VANELESS CONTRA-ROTATING STAGE

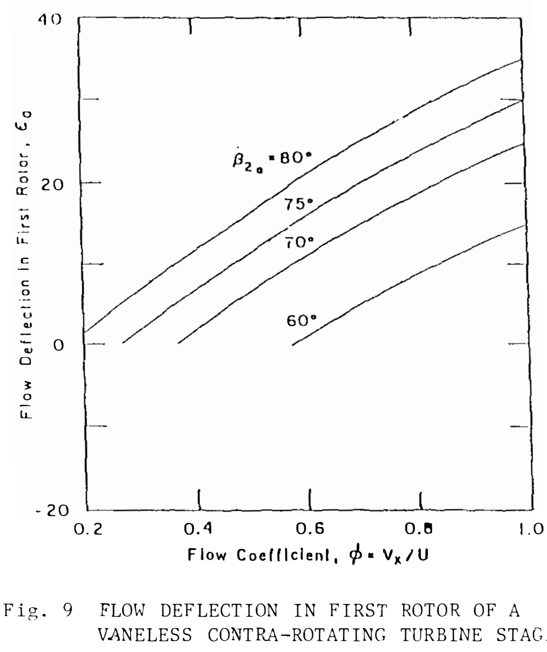

Fig. 9 FLOW DEFLECTION IN FIRST ROTOR OF A VANELESS CONTRA-ROTATING TURBINE STAGE

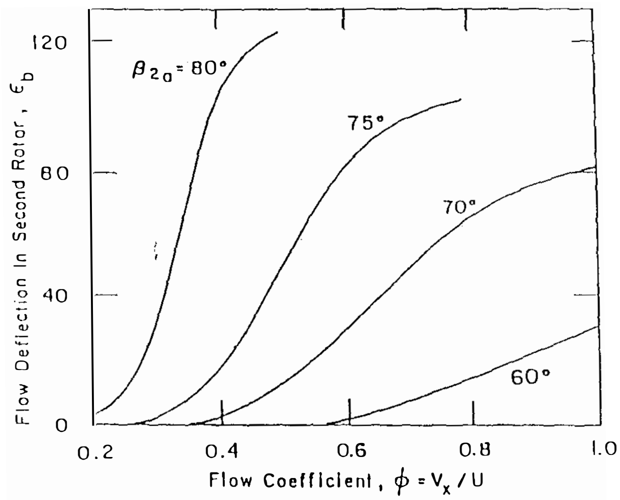

Fig. 10 FLOW DEFLECTION IN THE SECOND ROTOR OF A VANELESS CONTRA-ROTATING TURBINE STAGE

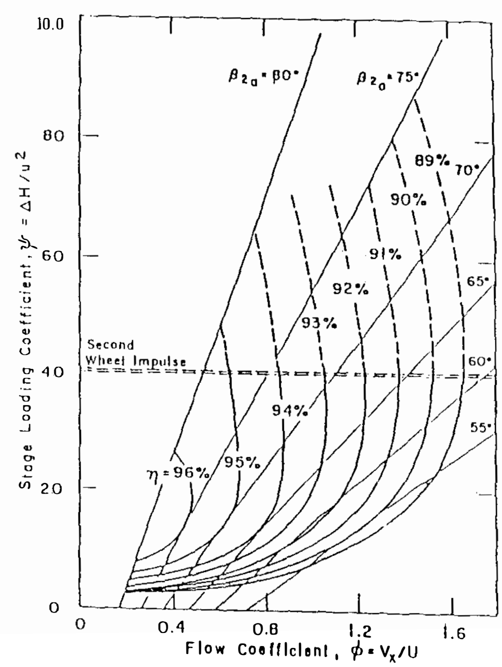

Fig. 11 CHART OF THE STAGE LOADING COEFFICIENT AND EFFICIENCY AS A FUNCTION OF THE FLOW COEFFICIENT